



Published in final edited form as:

ACS Nano. 2008 July ; 2(7): 1403–1410. doi:10.1021/nn800280r.

## Quantum Dot-Amphipol Nanocomplex for Intracellular Delivery and Realtime Imaging of siRNA

Lifeng Qi and Xiaohu Gao\*

Department of Bioengineering, University of Washington, William H. Foege Building N530M, Campus Box 355061, Seattle, WA 98195, USA.

### Abstract

A new generation of nanoparticle carrier that allows efficient delivery and real-time imaging of siRNA in live cells has been developed by combining two distinct types of nanomaterials, semiconductor quantum dots and amphipols. An important finding is that although amphipols are broadly used for solubilizing and delivering hydrophobic proteins into the lipid bilayers of cell membrane, when combined with nanoparticles, they offer previously undiscovered functionalities including cytoplasm delivery, siRNA protection, and endosome escape. Compared with the classic siRNA carriers such as Lipofectamine™ and polyetheleneimine, this new class of nanocarrier works in both serum-free and complete cell culture media, which is advantageous over Lipofectamine. It also outperforms polyethyleneimine in gene silencing under both conditions with significantly reduced toxicity. Furthermore, the intrinsic fluorescence of quantum dots provides a mechanism for real-time imaging of siRNA delivery in live cells. This new multifunctional, compact, and traceable nanocarrier is expected to yield important information on rational design of siRNA carriers and to have widespread applications of siRNA delivery and screening *in vitro* and *in vivo*.

### Keywords

nanoparticles; siRNA; amphipol; quantum dots; delivery; imaging

RNA interference (RNAi) is emerging as one of the most powerful technologies for sequence-specific suppression of genes and has potential applications ranging from functional gene analysis to therapeutics.<sup>1–8</sup> Due to the relatively low immunogenic and oncologic effects, the development of non-viral delivery methods *in vitro* and in organisms is of considerable current interest. In recent years, a number of strategies have been developed based on liposomes, gold and silica nanoparticles (NPs), cationic and biodegradable polymers, and peptides.<sup>9–19</sup> The delivery efficiency, however, remains low, especially under *in vivo* conditions. Another limitation shared by all the existing delivery technologies is the lack of an intrinsic signal for long term and real-time imaging of siRNA transport and release. Such imaging could provide important information on rational design of siRNA carriers. Currently, organic fluorophores are used to label siRNA or the delivery vehicles.<sup>13, 20, 21</sup> But the photobleaching problem associated with essentially all organic dyes prevents long-term tracking of siRNA-carrier complexes. Similarly, electron-dense gold NPs are visible under transmission electron microscope (TEM) and provide the highest imaging resolution in fixed cells, but they do not allow real-time imaging of live cells.

\*xgao@u.washington.edu.

Supporting Information Available: Stability of the QD-PMAL, electrophoresis detection limit of siRNA, and fluorescence quenching of FITC-siRNA by QDs. This material is available free of charge via the Internet at <http://pubs.acs.org>.

In this context, the use of semiconductor quantum dots (QDs) to study siRNA delivery in cells and small animals should be an excellent choice because of QDs' intrinsic fluorescence and their unique optical properties (*e.g.*, tunable emission, photostability and brightness). Indeed, recent work by Bhatia and co-workers has used QDs for siRNA delivery and imaging,<sup>22,23</sup> but the QD probes are either mixed with conventional siRNA delivery agents (Lipofectamine)<sup>22</sup> or external endosomal rupture compounds (*e.g.*, chloroquine) for gene silencing activity,<sup>23</sup> significantly limiting their potential applications *in vivo*. Therefore, development of multifunctional QDs with integrated functionalities of cell binding and internalization, endosome escape, siRNA protection against enzyme activities, siRNA unpackaging (siRNA-carrier dissociation), and siRNA tracking is of urgent need. On the other hand, packaging these functionalities into single nanoparticles also represents a significant technological challenge.

Here, we report a new technology by combining QDs with another class of nanomaterial, amphipol, to solve the aforementioned problems. Amphipols are linear polymers with alternating hydrophilic and hydrophobic side chains. They are widely used for solubilizing integral membrane proteins and delivering them into cell lipid bilayers (Figure 1a).<sup>24–28</sup> Unlike detergent-based micelles, amphipols belt around the transmembrane domain of membrane proteins and do not disrupt the integrity of cell membrane during delivery. To our surprise, however, when amphipols are mixed with nanoparticles coated with hydrophobic surface ligands, these two types of nanomaterials form stable complexes that are not only capable of carrying siRNA molecules into cytoplasm but also protecting them from enzymatic degradation (Figure 1b). In addition, the QDs should also provide a bright and stable fluorescent signal for intracellular siRNA imaging, since great success has been achieved in the past 5 years in using QDs for cellular staining and imaging.<sup>29–34</sup> The QD-amphipol technology reported here will open new opportunities for traceable intracellular delivery of siRNA without the need of additional compounds.<sup>35</sup>

## RESULTS AND DISCUSSION

In this report, we selected poly(maleic anhydride-alt-1-decene) modified with dimethylamino propylamine (PMAL, *m.w.* 18.5K) because of its multiple useful properties (Figure 1c). First, the hydrocarbons in PMAL bind to the hydrocarbons on the surface of QDs via multivalent hydrophobic interactions, leading to the formation of stable and water-soluble organic-inorganic hybrid structures (Figure 1d). Second, at neutral pH, the overall surface charge of the hybrid structure is highly positive, which allows immobilization of negatively charged biomolecules (*e.g.*, siRNAs) and interaction with negatively charged cell surface. Previously, we and others have prepared amphiphilic copolymers for QD solubilization and bioconjugation for cell labeling.<sup>29,36–38</sup> But all those polymers employ a dense layer of carboxylic acids, which prevents interaction with siRNA molecules. Third, the clustered tertiary amines grafted on the PMAL backbone have strong proton absorbing capability inside acidic cellular compartments such as endosomes, leading to osmotic swelling and endosome rupture.<sup>16,39–41</sup> Besides the tertiary amines, it has also been shown that the *pKa* of carboxylic acid groups in polymaleic anhydrides is also around 5 to 6, resulting in a second chemical group for proton absorption.<sup>42</sup> Fourth, the co-existence of tertiary amine and carboxylic acid groups weakens the interaction between siRNA and nanoparticles, which is expected to facilitate siRNA release inside cells. Indeed, it has been found that when polyethylenimine (PEI) are chemically modified to reduce electrostatic binding, the gene delivery activity is increased by 20–60 fold.<sup>43</sup> Furthermore, the zwitterionic surface of QD-PMAL could also become an important feature for *in vivo* applications, because zwitterionic charge reduces serum protein adsorption onto NP surface, which not only slows NP uptake by the reticuloendothelial systems (RES), but also helps NP renal clearance when the particles are made smaller than 5.5 nm.<sup>44, 45</sup>

The PMAL encapsulated QDs were prepared by a molecular self-assembly approach. QDs coated with hydrophobic ligands (tri-*n*-octylphosphine oxide or TOPO) were mixed with PMAL at a molar ratio of 1:500. Because of the strong multivalent hydrophobic interactions between TOPO and the PMAL hydrocarbons, QD and PMAL bind to each other and form highly stable complexes (at least 6 months, Supplementary Figure S1). Transmission electron microscopy (TEM), dynamic light scattering (DLS), and spectroscopy measurements were taken to thoroughly characterize the size and optical properties of purified QD-PMAL and its siRNA complex. The PMAL encapsulated QDs have excellent optical properties and narrow size distributions, with comparable quantum yield values as that of the original dots suspended in chloroform (Figure 2a). Dynamic light scattering measurements (Figure 2b) shows that QD-PMAL has a hydrodynamic diameter of  $12.1 \pm 1.5$  nm (1.5 nm is the standard deviation of three different samples, rather than the size spread in one sample). Considering the QD core is  $5.5 \pm 0.7$  nm in diameter (Figure 2c), the larger hydrodynamic radius in aqueous buffers is likely due to the physical size of the positively-charged PMAL polymer, as well as its strong interaction with the solvent.<sup>46</sup> This surface charge is sufficient to carry small oligonucleotides and deliver them into mammalian cells. When bind to siRNA, the size of the nanoparticle complexes further increases to  $15.9 \pm 1.0$  nm (1.0 nm is the standard deviation of three different samples), suggesting that QDs remain mainly single with siRNA on the surface, a result that was also confirmed by the 'blinking' feature of QDs under fluorescence microscopy. The compact size of single particles is highly desirable because large particles enter cells at a much slower rate,<sup>47</sup> and can be eliminated quickly by the RES system *in vivo*.<sup>48</sup> In contrast, previously reported gene deliveries based on silica and gold nanoparticles often form 100–200 nm aggregates likely because the size mismatch of large plasmid DNA to small nanoparticles, and consequently it requires many NPs to work together (forming clusters with the DNA plasmid) for successful transfection.<sup>10–13</sup>

To investigate the number of siRNAs that can be loaded onto individual QDs, we labeled siRNA molecules with FITC dye (green) and mixed the siRNA (constant siRNA quantity at 10 pmol) with red QDs at various molar ratios. As shown in the gel electrophoresis data (Figure 3a), the fluorescence intensity of the siRNA band gradually decreases as QD concentration increases, and disappears when the siRNA/QD ratio is below 10, indicating that approximately 10 siRNA molecules can be immobilized onto the surface of individual QDs. To ensure this result is not an artifact due to the detection limit of gel electrophoresis, siRNA-FITC samples of various quantity ranging from 10 – 0.1 pmol were also studied under similar experiment conditions. As shown in Supplementary Figure S2, siRNA of 0.2 pmol is still detectable, suggesting that the disappearance of siRNA bands in the siRNA/QD ratio studies is indeed due to siRNA-QD binding. Focused on the siRNA/QD ratio of 1:1, which is used in the siRNA intracellular delivery experiment described below, two additional assays were conducted to confirm siRNA-QD association. First, zeta potential measurements show that QD-PMAL has a zeta potential value of 21.3 mV before siRNA binding and it reduces to 18.2 mV after siRNA binding, because negatively charged siRNA partially neutralizes the positive charge on QD surface. Second, the interaction of siRNA to QDs can also be characterized by fluorescence quenching of FITC-labeled siRNA due to fluorescence resonance energy transfer or FRET (Supplementary Figure S3).

The association of siRNA to QDs provides a mechanism for siRNA protection against enzymatic degradation. This is a very important feature because RNAs in general are susceptible to nuclease digestion. Enhanced resistance to nuclease degradation should increase siRNA lifetime in the cell and the subsequent interference effect on target mRNAs. Gel electrophoresis experiments show that QD-bound siRNAs are degraded at a significantly slower rate (75% intact) compared with free siRNA (undetectable) under the same experiment conditions (Figure 3b). Similar results have been previously observed with plasmid DNA and

short oligonucleotides on silica and gold NPs, and have been attributed to the NP steric hindrance to nuclease activities.<sup>49–53</sup>

To evaluate the RNAi efficiency using QD-PMAL delivery vehicle, a model gene silencing experiment was designed using human breast adenocarcinoma cell line (SK-BR-3) and siRNA targeting Her-2/neu. Her-2/neu, a cell surface receptor tyrosine kinase, is over-expressed in approximately 30% of breast tumors, and is an excellent model system because it is involved in signal transduction pathways leading to cell growth and differentiation. Figure 4 shows that Her-2/neu expression was suppressed to  $36\pm 2\%$  using QD-PMAL in serum-free media. In comparison, when the two common transfection reagents (Lipofectamine and PEI) are used, the target gene expression was reduced to  $29\pm 5\%$  and  $58\pm 13\%$ , respectively. When used in complete cell culture media (contains serum), QD-PMAL reduces Her-2 expression to  $35\pm 4\%$ , similar to the values achieved with serum-free media. Lipofectamine and PEI reduce Her-2 expression to  $48\pm 7\%$  and  $62\pm 5\%$ . These results demonstrate that QD-PMAL is efficient in siRNA intracellular delivery for both serum-free and complete media. In contrast, Lipofectamine only works well in serum-free media, and the QD-PMAL also outperforms PEI under both conditions.

The high delivery efficiency of QD-PMAL could be explained by its structural and surface properties. First, when form complexes with siRNA, QDs remain single, and the small sizes facilitate their diffusion and entry into cells. Secondly, after the nanostructures are endocytosed, both the tertiary amines and carboxylic groups on QD surface play important roles in endosome escape. At low pH values carboxylic and amine groups are protonated, and at high pH values they will be deprotonated. Therefore, the zwitterionic surface behaves like a buffer system that can quickly neutralize excess protons in endosome, which also lead to a net influx of chloride ions. The osmotic pressure building along this proton buffering process will eventually rupture the endosomes, a process known as ‘proton sponge effect’.<sup>16, 39–41</sup>

Owing to the intrinsic fluorescence of QDs, the intracellular behavior of QD-siRNA complexes including cell entry, endosome escape, and transport can be monitored in real-time. Time-lapse confocal microscopy (Figure 5) shows that the QD-siRNA complexes attach to cell surface immediately after mixing with cells (a bright ring structure). Subsequent incubation over a period of 1 hour allows the complexes to enter and accumulate inside cells (bright interior), suggesting efficient transport across the plasma membrane. During this period, only the QD fluorescence (red) is visible, but not the siRNA-FITC (green), indicating that siRNA and QDs are associated to each other (FITC is quenched due to FRET). The siRNA molecules started to separate from QDs as soon as 1.5 hours (signal appeared in the green channel). More importantly, after 5 hour incubation, siRNAs became evenly distributed in the cytoplasm, confirming the efficient endosome escape. It’s also interesting to note that the QDs are not evenly distributed in the cytoplasm after endosome rupture. Instead, they form large clusters, likely due to aggregation with intracellular proteins and lipids. When this process was performed *in vitro* by acidifying the buffer to pH 5, siRNA and QDs remain single and bound, suggesting that inside cells siRNA are likely replaced from QD surface by other biomolecules. It’s also worth mentioning that the characteristic intermittent fluorescence of QDs does not interfere with fluorescence imaging in the current study, because QDs are imaged in groups. After the QD-siRNAs enter cells through endocytosis, many copies of the complexes are confined in small endosomal compartments. Although individual QDs fluoresce in an on-and-off manner, the chance that multiple copies of QDs stay in the ‘dark’ state simultaneously is extremely small. Collectively, QDs remain in the ‘bright’ state at all time.

A remaining key question is whether QD-PMAL as a new siRNA carrier is toxic to cells. This is a particularly important issue when the core nanoparticle is a semiconductor QD, because it contains cadmium. However, our results show that QDs are nearly non-toxic to cells, whereas

Lipofectamine and PEI reduce cell viability to 84% and 68%, respectively. The low toxicity of QDs is perhaps not surprising because the stable PMAL polymer coating layer protects QDs from exposing to the intracellular environment and thereby prevents Cd<sup>2+</sup> release. Indeed, the QDs remain highly fluorescent even in acidic endosomes, indicating that the core QDs are intact. In contrast, when siRNA targeting Her-2 was used in the study, the QD-siRNA was found toxic to cells, demonstrated by a greater than 20% decrease in cell viability. This siRNA toxicity was minimal when scramble siRNA sequence was used. Similar result was also observed with Lipofectamine transfection. The cell death triggered by Her-2 siRNA also confirms successful gene silencing, because Her-2 is involved in signaling pathways of cell growth and differentiation. It has been previously shown that knockdown of Her-2/neu gene in SK-BR-3 cells inhibits cell proliferation and induces apoptosis.<sup>54</sup> We also noticed that the Her-2 siRNA toxicity and the level of Her-2 silencing only correlate qualitatively, indicating the Her-2 siRNA toxicity and Her-2 silencing may not have a linear relationship. Quantitative measurement of the Her-2 siRNA cytotoxicity effect deserves further investigation. For potential translational and clinical applications of this technology, the suitability of using QDs is difficult to predict at this time because the long-term (*e.g.*, years) toxicity of QDs is largely unknown. However, it's also important to point out that the core particle is not limited to QDs for nanoparticle-PMAL assembly. Traceable nanoparticles with non- or minimum-toxic chemical elements (such as silicon and iron oxides) can be used and encapsulated with PMAL using similar chemistry.

## CONCLUSION

We have developed a new siRNA delivery technology by integrating two distinct types of nanomaterials, semiconductor QDs and amphipols. An important finding is that although amphipols have found widespread uses in solubilizing and delivering hydrophobic proteins into the cell lipid bilayers, when combined with nanoparticles, they offer previously undiscovered functionalities including siRNA cytoplasm delivery, siRNA protection, and endosome escape. Compared with the traditional siRNA carriers such as Lipofectamine and PEI, this new class of nanocarrier delivers siRNA into cancer cells efficiently in both serum-free and complete media with significantly reduced cytotoxicity. Furthermore, the unique optical properties of QDs and exquisite design of imaging assays (such as FRET) allow real-time imaging of siRNA delivery in live cells. We envision that further development of this new multifunctional, compact, and traceable nanocarrier (such as incorporating a targeting probe) will enable new developments in siRNA discovery and delivery, functional genomics, gene therapy, as well as biophysical studies.

## MATERIALS AND EXPERIMENTS

Unless specified, chemicals were purchased from Sigma-Aldrich (St. Louis, MO) and used without further purification. PMAL was purchased from Anatrace Inc. (Maumee, OH). siRNA targeting Her-2, FITC labeled siRNA targeting Her-2, and the control sequence were purchased from Ambion (Austin, Tx). A UV-2450 spectrophotometer (Shimadzu, Columbia, MD) and a Fluoromax4 fluorometer (Horiba Jobin Yvon, Edison, NJ) were used to characterize the absorption and emission spectra of QDs. A tabletop ultracentrifuge (Beckman TL120) was used for nanoparticle purification and isolation. The dry and hydrodynamic radii of QDs were measured on a CM100 transmission electron microscope (Philips EO, Netherlands) and a nanoparticle size analyzer (NanoZS, Worcestershire, United Kingdom). Confocal fluorescence images were obtained with a confocal microscope (Zeiss LSM 510, Germany) equipped with DPSS, Argon, and He/Ne lasers with lines at 405, 458, 488, 543, and 633 nm. Multicolor gel images were acquired with a macro-imaging system (Lightools Research, Encinitas, CA). For the cytotoxicity measurements based on MTT assay, a Tecan Safire<sup>2</sup> plate reader (Switzerland) was used.



## PREPARATION AND CHARACTERIZATION OF QD-PMAL COMPLEX

Highly luminescent QDs were synthesized as previously described by Peng and coworkers.<sup>55, 56</sup> Briefly, CdO (1 mmol) was dissolved in 1 g stearic acid with heating. After formation of a clear solution, a mixture of tri-n-octylphosphine oxide (TOPO, 5 g) and hexadecylamine (HDA, 5 g) was added as the reaction solvent, which was then heated to 250 °C under argon for 10 minutes. The reaction temperature was briefly raised to 350 °C, and equal molar Se is quickly injected into the hot solvent. The reaction immediately changes color to orange-red, indicating QD formation. The dots were refluxed for 10 minutes, and capping solution of 20 mM dimethylzinc and hexamethyldisilathiane was slowly added to protect the CdSe core. The resulting QDs were cooled to room temperature, and rinsed repeatedly with methanol and hexane mixture to remove free ligands. UV adsorption, fluorescence emission spectroscopy, TEM, and DLS were used for characterization of particle optical properties and sizes.

For QD-PMAL complex preparation, 10 mg PMAL was mixed with 1 nmol of QDs in chloroform. The solvent was then allowed to slowly dry in air, leading to the formation a thin film of QD-PMAL complexes. The dried film was dissolved in 50 mM borate buffer (pH 8.5) with agitation or sonication. Free PMAL polymers (unbound polymers) were removed by ultracentrifugation (45,000 rpm for 50 min). The fluorescence absorption and emission, the nanoparticle dry size and dynamic radii, surface charge, and electrophoretic mobility of the resulting nanoparticles were measured.

## SIRNA LOADING CAPACITY (NUMBER OF SIRNA PER QD)

FITC-labeled siRNA targeting Her-2 (10 pmol) was incubated for 20 min with QDs of 10, 1, 0.5, 0.33, 0.25, and 0.2 pmol to achieve siRNA/QD molar ratios of 1:1, 1:10, 1:20, 1:30, 1:40, and 1:50. Electrophoresis and fluorescence imaging were then used to separate and quantify the unbound siRNA. To probe the detection limit of the gel electrophoresis technique, siRNAs of various concentrations were also studied.

## SIRNA PROTECTION BY QDS

For siRNA stability studies, siRNA-QD complexes (1  $\mu$ M) or siRNA alone were incubated with ribonuclease (25ng, Fisher Scientific, Pittsburgh, PA). The enzyme digestion reaction was stopped at 30 min by inactivating the nuclease with ribonuclease inhibitor (Promega, Madison, WI). The siRNA molecules were then released from the surface of QDs using 1% SDS. Electrophoresis was again used to quantify the intact siRNAs.

## IN VITRO SIRNA DELIEVERY

siRNA transfection was performed with QD-PMAL, and for comparison, with Lipofectamine 2000 (Invitrogen, Carlsbad, CA) and PEI (*m.w.* 25 kDa). Briefly,  $5 \times 10^4$  cells/well were plated into 24-well plates overnight to achieve 60–80% confluence. On the day of transfection, cultured cells were washed and pre-incubated for 40 min with 500  $\mu$ l/well OptiMEM media (Invitrogen, Carlsbad, CA). 20 pmol siRNA targeting Her-2/neu was diluted into 50  $\mu$ l OptiMEM. For siRNA transfection with Lipofectamine, 1  $\mu$ l/well transfection reagent (following vendor's protocol) was diluted into 50  $\mu$ l of OptiMEM, incubated for 10 min at room temperature, and mixed with siRNA. The complexes were added into cell culture to reach a siRNA final concentration of 33 nM. For siRNA transfection with PEI, the same concentration of siRNA (33 nM) and an N/P ratio of 14 were used. For transfection with PMAL encapsulated QDs, 20 pmol of QDs and siRNA were mixed in OptiMEM (100  $\mu$ l), incubated for 20 min, and then added into cell culture media (500  $\mu$ l serum-free OptiMEM or complete RPMI) to achieve a final QD-siRNA concentration of 33 nM.

## IMMUNO-BLOTTING

Transfected cells were lysed using RIPA lysis buffer containing 1% Igepal-630, 0.5% deoxycholate, 0.1% SDS, 1 mM PMSF and 1  $\mu\text{g/ml}$  each of leupeptin, aprotinin and pepstatin in phosphate buffered saline (PBS). After centrifugation, the supernatant of the cell lysate was collected and the protein was measured by the standard Bradford assay (Bio-Rad laboratories, Inc. Hercules, CA). Equal amounts of protein were loaded and separated on 10% SDS-PAGE then transferred to nitrocellulose membranes and blocked with 5% milk blocking buffer for 2h. The membrane was incubated with rabbit polyclonal anti-human Her-2/neu antibodies (Abcam, Cambridge, MA), washed in Tween-Tris Buffered Saline (TTBS: 0.1% Tween-20 in 100 mM Tris-CL [pH 7.5], 0.9% NaCl), and probed with HRP-linked labeled goat anti-rabbit secondary antibodies (Abcam, Cambridge, MA). The blot was developed using an ECL kit (Pierce, Rockford, IL). Digital chemiluminescent images of the membrane were recorded using KODAK Image Station 4000MM.  $\beta$ -actin was probed in the same way (except the antibodies) as the protein loading control.

## CYTOTOXICITY EVALUATION

Standard MTT assay<sup>57</sup> was performed to determine the cytotoxicity of the transfection agents and their siRNA complexes. Briefly, cells were incubated with the transfection agents for 24 hours, collected by trypsinization, counted, and plated at a density 20,000 cells/well in 96-well flat-bottomed microtiter plates (100  $\mu\text{l}$  of cell suspension/well). Each siRNA delivery agent was investigated with or without siRNA. The absorbance of the converted dye was measured at a wavelength of 570nm. The experiments were repeated at least three times.

## Supplementary Material

Refer to Web version on PubMed Central for supplementary material.

## Acknowledgments

This work was supported in part by NIH, NSF, the Seattle Foundation, and the Department of Bioengineering at the University of Washington. X.G. thanks the NSF for a Faculty Early Career Development award (CAREER). We are especially grateful to P.S. Stayton, A.S. Hoffman, S. Pun and M. Zhang for uses of their particle sizer and gel documentation system, G. Martin at the UW Keck Imaging Center for help with confocal microscopy, T.J. Kavanagh and D.L. Eaton for fruitful discussion on nanotoxicity, and Y.A. Wang at Oceananotech for help with QD synthesis.

## References

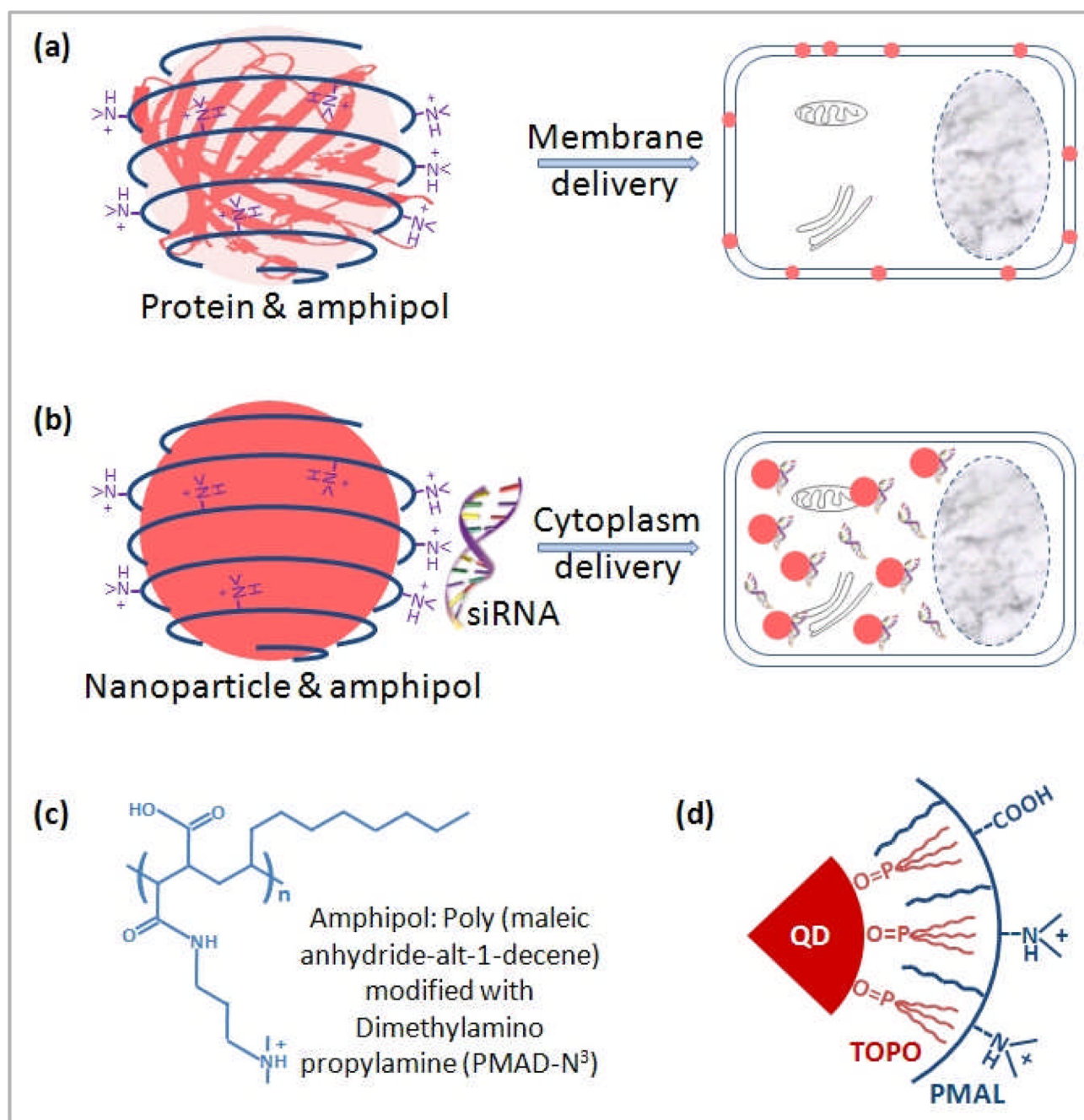
1. Hannon GJ. RNA Interference. *Nature* 2002;418:244–251. [PubMed: 12110901]
2. Scherer LJ, Rossi JJ. Approaches for The Sequence-Specific Knockdown of mRNA. *Nat. Biotechnol* 2003;21:1457–1465. [PubMed: 14647331]
3. Dykxhoorn DM, Novina CD, Sharp PA. Killing the Messenger: Short RNAs that Silence Gene Expression. *Nat. Rev. Mol. Cell Biol* 2003;4:457–467. [PubMed: 12778125]
4. Kim DH, Rossi JJ. Strategies for Silencing Human Disease Using RNA Interference. *Nat. Rev. Genetics* 2007;8:173–182. [PubMed: 17304245]
5. Rana TM. Illuminating the Silence: Understanding the Structure and Function of Small RNAs. *Nat. Rev. Mol. Cell Biol* 2007;8:23–36. [PubMed: 17183358]
6. Bumcrot D, Manoharan M, Kotliansky V, Sah DW. RNAi Therapeutics: A Potential New Class of Pharmaceutical Drugs. *Nat. Chem. Biol* 2006;2:711–719. [PubMed: 17108989]
7. Meister G, Tuschl T. Mechanisms of Gene Silencing by Double-Stranded RNA. *Nature* 2004;431:343–349. [PubMed: 15372041]
8. Dykxhoorn DM, Lieberman J. The Silent Revolution: RNA Interference as Basic Biology, Research Tool, and Therapeutic. *Ann. Rev. Med* 2005;56:401–423. [PubMed: 15660519]

9. Chesnoy S, Huang L. Structure and Function of Lipid-DNA Complexes for Gene Delivery. *Annu. Rev. Biophys. Biomol. Struct* 2000;29:27–47. [PubMed: 10940242]
10. Sandhu KK, McIntosh CM, Simard JM, Smith SW, Rotello VM. Gold Nanoparticle-Mediated Transfection of Mammalian Cells. *Bioconjug. Chem* 2002;13:3–6. [PubMed: 11792172]
11. Niidome T, Nakashima K, Takahashi H, Niidome Y. Preparation of Primary Amine-Modified Gold Nanoparticles and Their Transfection Ability into Cultivated Cells. *Chem. Commun* 2004;7:1978–1979.
12. Kneuer C, Sameti M, Bakowsky U, Schiestel T, Schirra H, Schmidt H, Lehr CM. A Nonviral DNA Delivery System Based on Surface Modified Silica-Nanoparticles Can Efficiently Transfect Cells *In Vitro*. *Bioconjug. Chem* 2000;11:926–932. [PubMed: 11087343]
13. Roy I, Ohulchanskyy TY, Bharali DJ, Pudavar HE, Mistretta RA, Kaur N, Prasad PN. Optical Tracking of Organically Modified Silica Nanoparticles as DNA Carriers: A Nonviral, Nanomedicine Approach for Gene Delivery. *Proc. Natl. Acad. Sci. USA* 2005;102:279–284. [PubMed: 15630089]
14. Rudolph C, Plank C, Lausier J, Schillinger U, Müller RH, Rosenecker J. Oligomers of The Arginine-Rich Motif of The HIV-1 TAT Protein are Capable of Transferring Plasmid DNA into Cells. *J. Biol. Chem* 2003;278:11411–11418. [PubMed: 12519756]
15. Zanta MA, Belquise-Valladier P, Behr JP. Gene Delivery: A Single Nuclear Localization Signal Peptide is Sufficient to Carry DNA to The Cell Nucleus. *Proc. Natl. Acad. Sci. USA* 1999;96:91–96. [PubMed: 9874777]
16. Boussif O, Lezoualc'h F, Zanta MA, Mergny MD, Scherman D, Demeneix B, Behr JP. A Versatile Vector for Gene and Oligonucleotide Transfer into Cells in Culture and *In Vivo*: Polyethylenimine. *Proc. Natl. Acad. Sci. USA* 1995;92:7297–7301. [PubMed: 7638184]
17. Bielinska AU, Chen C, Johnson J, Baker JR Jr. DNA Complexing with Polyamidoamine Dendrimers: Implications for Transfection. *Bioconjug. Chem* 1999;10:843–850. [PubMed: 10502352]
18. Tang MX, Redemann CT, Szoka FC Jr. *In Vitro* Gene Delivery by Degraded Polyamidoamine Dendrimers. *Bioconjug. Chem* 1996;7:703–714. [PubMed: 8950489]
19. Takeshita T, Minakuchi T, Nagahara S, Honma K, Sasaki H, Hirai K, Teratani T, Namatame N, Yamamoto Y, Hanai K, et al. Efficient Delivery of Small Interfering RNA to Bone-metastatic Tumors by Using Atelocollagen *In Vivo*. *Proc. Natl. Acad. Sci. USA* 2005;102:12177–12182. [PubMed: 16091473]
20. Kulkarni RP, Wu DD, Davis ME, Fraser SE. Quantitating Intracellular Transport of Polyplexes by Spatio-Temporal Image Correlation Spectroscopy. *Proc. Natl. Acad. Sci. USA* 2005;102:7523–7528. [PubMed: 15897455]
21. Suh J, Wirtz D, Hanes J. Efficient Active Transport of Gene Nanocarriers to the Cell Nucleus. *Proc. Natl. Acad. Sci. USA* 2003;100:3878–3882. [PubMed: 12644705]
22. Chen AA, Derfus AM, Khetani SR, Bhatia SN. Quantum Dots to Monitor RNAi Delivery and Improve Gene Silencing. *Nucleic Acids Res* 2005;33:e190.
23. Derfus AM, Chen AA, Min DH, Ruoslahti E, Bhatia SN. Targeted Quantum Dot Conjugates for siRNA Delivery. *Bioconjug. Chem* 2007;18:1391–1396. [PubMed: 17630789]
24. Gorzelle BM, Hoffman AK, Keyes MH, Gray DN, Ray DG, Sanders CR. Amphipols Can Support the Activity of A Membrane Enzyme. *J. Am. Chem. Soc* 2002;124:11594–11595. [PubMed: 12296714]
25. Tribet C, Audebert R, Popot JL. Amphipols: Polymers that Keep Membrane Proteins Soluble in Aqueous Solutions. *Proc. Natl. Acad. Sci. USA* 1996;93:15047–15050. [PubMed: 8986761]
26. Pocanschi CL, Dahmane T, Gohon Y, Rappaport F, Apell HJ, Kleinschmidt JH, Popot JL. Amphipathic Polymers: Tools to Fold Integral Membrane Proteins to Their Active Form. *Biochemistry* 2006;45:13954–13961. [PubMed: 17115690]
27. Tribet C, Audebert R, Popot JL. Stabilization of Hydrophobic Colloidal Dispersions in Water with Amphiphilic Polymers: Applications to Integral Membrane Proteins. *Langmuir* 1997;13:5570–5576.
28. Nagy JK, Kuhn Hoffmann A, Keyes MH, Gray DN, Oxenoid K, Sanders CR. Use of Amphipathic Polymers to Deliver a Membrane Protein to Lipid Bilayers. *FEBS Lett* 2001;501:115–120. [PubMed: 11470268]



29. Wu XY, Liu HJ, Liu JQ, Haley KN, Treadway JA, Larson JP, Ge NF, Peale F, Bruchez MP. Immunofluorescent Labeling of Cancer Marker Her2 and Other Cellular Targets with Semiconductor Quantum Dots. *Nat. Biotechnol* 2003;21:41–46. [PubMed: 12459735]
30. Jaiswal JK, Mattoussi H, Mauro JM, Simon SM. Long-Term Multiple Color Imaging of Live Cells Using Quantum Dot Bioconjugates. *Nat. Biotechnol* 2003;21:47–51. [PubMed: 12459736]
31. Dahan M, Lévi S, Luccardini C, Rostaing P, Riveau B, Triller A. Diffusion Dynamics of Glycine Receptors Revealed by Single-Quantum Dot Tracking. *Science* 2003;302:442–445. [PubMed: 14564008]
32. Medintz IL, Uyeda HT, Goldman ER, Mattoussi H. Quantum Dot Bioconjugates for Imaging, Labeling and Sensing. *Nat. Mater* 2005;4:435–436. [PubMed: 15928695]
33. Yezhelyev MV, Al-Hajj A, Morris C, Marcus AI, Liu TR, Lewis M, Cohen C, Zrazhevskiy P, Simons JW, Rogatko A, et al. In situ Molecular Profiling of Breast Cancer Biomarkers with Multicolor Quantum Dots. *Adv. Mater* 2007;19:3146–3151.
34. Smith AM, Dave S, Nie S, True L, Gao X. Multicolor Quantum Dots for Molecular Diagnostics of Cancer. *Expert Rev. Mol. Diagn* 2006;6:231–244. [PubMed: 16512782]
35. Qi L, Gao X. Emerging Application of Quantum Dots for Drug Delivery and Therapy. *Expert Opin. Drug Deliv* 2008;5:263–267. [PubMed: 18318649]
36. Gao X, Cui Y, Levenson RM, Chung LW, Nie S. *In Vivo* Cancer Targeting and Imaging with Semiconductor Quantum Dots. *Nat. Biotechnol* 2004;22:969–976. [PubMed: 15258594]
37. Dubertret B, Skourides P, Norris DJ, Noireaux V, Brivanlou AH, Libchaber A. *In Vivo* Imaging of Quantum Dots Encapsulated in Phospholipid Micelles. *Science* 2002;298:1759–1762. [PubMed: 12459582]
38. Pellegrino T, Manna L, Kudera S, Liedl T, Koktysh D, Rogach AL, Keller S, Rädler J, Natile G, Parak WJ. Hydrophobic Nanocrystals Coated with an Amphiphilic Polymer Shell: a General Route to Water Soluble Nanocrystals. *Nano Lett* 2004;4:703–707.
39. Godbey WT, Wu KK, Mikos AG. Poly(ethylenimine) and its Role in Gene Delivery. *J. Control. Release* 1999;5:149–160. [PubMed: 10425321]
40. Sonawane ND, Szoka FC Jr, Verkman AS. Chloride Accumulation and Swelling in Endosomes Enhances DNA Transfer by Polyamine-DNA Polyplexes. *J. Biol. Chem* 2003;278:44826–44831. [PubMed: 12944394]
41. Haensler J, Szoka FC. Polyamidoamine Cascade Polymers Mediate Efficient Transfection of Cells in Culture. *Bioconjugate Chem* 1993;4:372–379.
42. Henry SM, El-Sayed ME, Pirie CM, Hofferma AS, Stayton PS. pH-Responsive Poly(styrene-alt-maleic anhydride) Alkylamide Copolymers for Intracellular Drug Delivery. *Biomacromolecules* 2006;7:2407–2414. [PubMed: 16903689]
43. Gabrielson NP, Pack DW. Acetylation of Polyethylenimine Enhances Gene Delivery via Weakened Polymer/DNA Interactions. *Biomacromolecules* 2006;7:2427–2435. [PubMed: 16903692]
44. Choi HS, Liu W, Misra P, Tanaka E, Zimmer JP, Itty Ipe B, Bawendi MG, Frangioni JV. Renal Clearance of Quantum Dots. *Nat. Biotechnol* 2007;25:1165–1170. [PubMed: 17891134]
45. Liu W, Choi HS, Zimmer JP, Tanaka E, Frangioni JV, Bawendi M. Compact Cysteine-Coated CdSe (ZnCdS) Quantum Dots for *In Vivo* Applications. *J. Am. Chem. Soc* 2007;129:14530–14531. [PubMed: 17983223]
46. Larson DR, Zipfel WR, Williams RM, Clark SW, Bruchez MP, Wise FW, Webb WW. Water-Soluble Quantum Dots for Multiphoton Fluorescence Imaging *In Vivo*. *Science* 2003;300:1434–1436. [PubMed: 12775841]
47. Jiang W, Kim BYS, Rutka JT, Chan WCW. Nanoparticle-Mediated Cellular Response is Size-Dependent. *Nat. Nanotechnol* 2008;3:145–150. [PubMed: 18654486]
48. Li W, Szoka FC Jr. Lipid-Based Nanoparticles for Nucleic Acid Delivery. *Pharm. Res* 2007;24:438–449. [PubMed: 17252188]
49. He XX, Wang K, Tan W, Liu B, Lin X, He C, Li D, Huang S, Li J. Bioconjugated Nanoparticles for DNA Protection from Cleavage. *J. Am. Chem. Soc* 2003;125:7168–7169. [PubMed: 12797777]
50. McIntosh CM, Esposito EA 3rd, Boal AK, Simard JM, Martin CT, Rotello VM. Inhibition of DNA Transcription Using Cationic Mixed Monolayer Protected Gold Clusters. *J. Am. Chem. Soc* 2001;123:7626–7629. [PubMed: 11480984]

51. Fischer NO, McIntosh CM, Simard JM, Rotello VM. Inhibition of Chymotrypsin through Surface Binding using Nanoparticle-Based Receptors. *Proc. Natl. Acad. Sci. USA* 2002;99:5018–5023. [PubMed: 11929986]
52. Bharali DJ, Klejbor I, Stachowiak EK, Dutta P, Roy I, Kaur N, Bergey EJ, Prasad PN, Stachowiak MK. Organically Modified Silica Nanoparticles: A Nonviral Vector for *In Vivo* Gene Delivery and Expression in the Brain. *Proc. Natl. Acad. Sci. USA* 2005;102:11539–11544. [PubMed: 16051701]
53. Rosi NL, Giljohann DA, Thaxton CS, Lytton-Jean AK, Han MS, Mirkin CA. Oligonucleotide-Modified Gold Nanoparticles for Intracellular Gene Regulation. *Science* 2006;312:1027–1030. [PubMed: 16709779]
54. Faltus T, Yuan J, Zimmer B, Krämer A, Loibl S, Kaufmann M, Strebhardt K. Silencing of the *HER2/neu* Gene by siRNA Inhibits Proliferation and Induces Apoptosis in *HER2/neu*-Overexpressing Breast Cancer Cells. *Neoplasia* 2004;6:786–795. [PubMed: 15720805]
55. Qu LH, Peng XG. Control of Photoluminescence Properties of CdSe Nanocrystals in Growth. *J. Am. Chem. Soc* 2002;124:2049–2055. [PubMed: 11866620]
56. Peng ZA, Peng XG. Formation of High-Quality CdTe, CdSe, and CdS Nanocrystals using CdO as Precursor. *J. Am. Chem. Soc* 2001;123:183–184. [PubMed: 11273619]
57. Truter EJ, Santos AS, Els WJ. Assessment of the Antitumor Activity of Targeted Immunospecific Albumin Microspheres Loaded with Cisplatin and 5-fluorouracil: Toxicity against a Rodent Ovarian Carcinoma *In Vitro*. *Cell Biol. Int* 2001;25:51–59. [PubMed: 11237408]

**Figure 1.**

Schematic drawing of the hybrid structure of QD and amphipol for siRNA delivery and real-time imaging in live cells. (a) Solubilization of hydrophobic proteins and delivery into cell membrane lipid bilayers.<sup>24</sup> (b) Hydrophobic QDs encapsulated by amphipol for siRNA intracellular delivery. The siRNA molecules are attached to the QD surface via electrostatic interaction. (c) Molecular structure of the amphipol polymer used in the current study. The polymer has both a hydrophobic domain (hydrocarbons) and a hydrophilic domain (carboxylic acids and tertiary amines). (d) Schematic drawing of the hydrophobic interaction between TOPO-coated QDs and the amphipol. The amphipol and QDs are bound to each other via multivalent hydrophobic interaction.

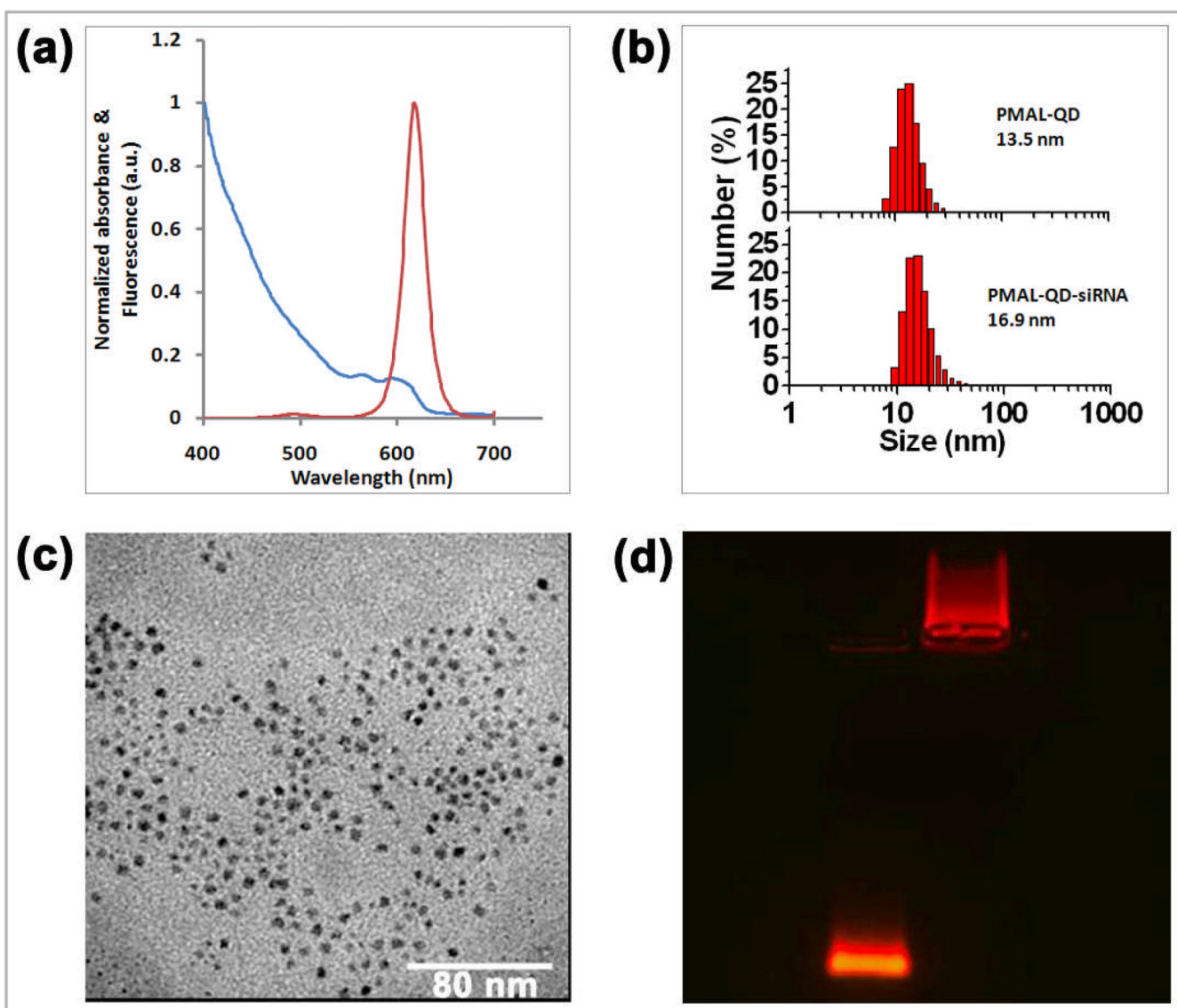


**Figure 2.** Characterization of the size, surface charge, and optical properties of QD-PMAL. (a) Fluorescence absorption and emission spectra; (b) hydrodynamic size of a representative sample measured by DLS; (c) QD core size measured by TEM; and (d) surface charges of PMAL coated QDs measured by gel electrophoresis in comparison with poly(maleic anhydride alt-tetradecene) (or PMAT) coated QDs, which is negatively charged because only carboxylic acids are present. The QDs have a core size of  $5.5 \pm 0.7$  nm measured by TEM, and a hydrodynamic diameter of  $12.1 \pm 1.5$  nm (a representative measurement of 13.5 nm is shown) before siRNA binding and  $15.9 \pm 1.0$  nm (a representative run showing 16.9 nm) after siRNA binding. The positive charge of QD-PMAL is also confirmed by the gel electrophoresis. The gel running buffer has a pH of 8.5. Under this condition, the QD-PMAL runs significantly slower than QD-PMAT.



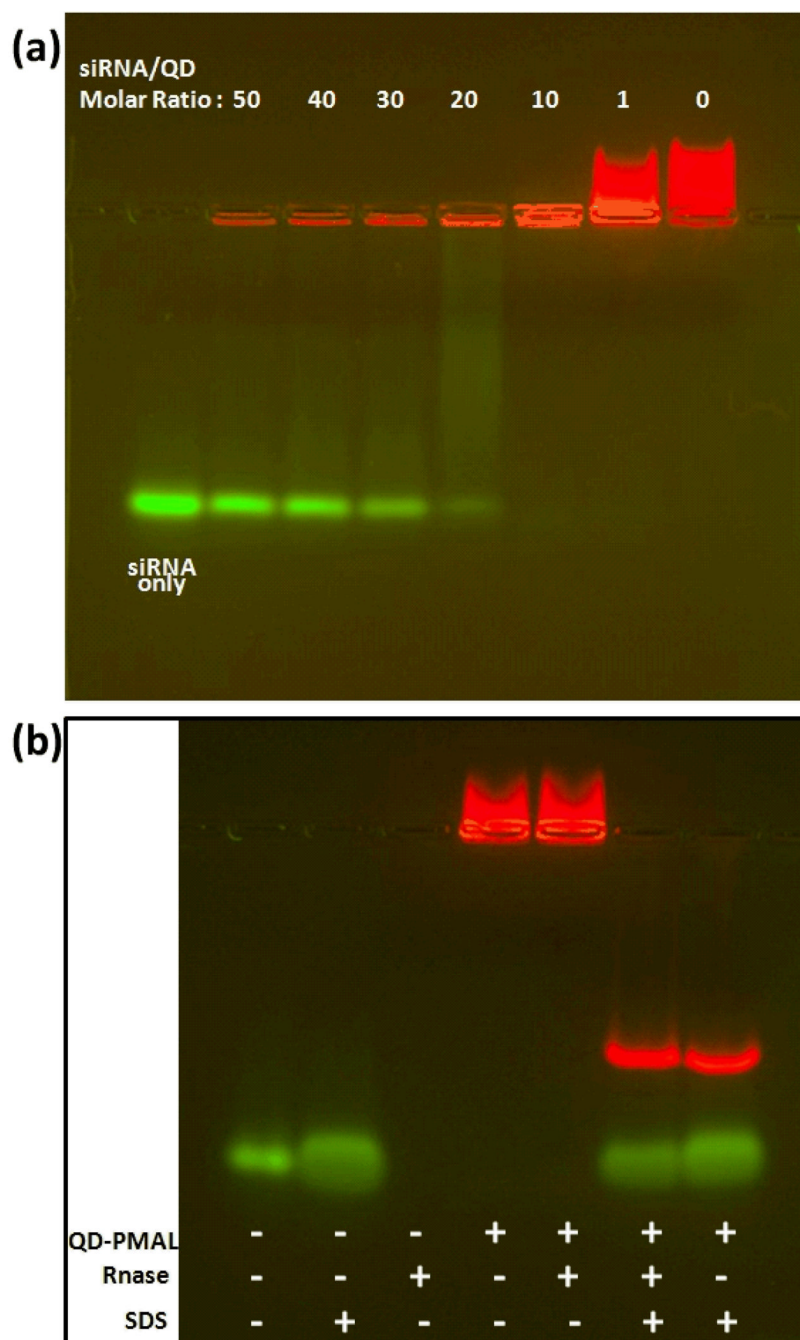


**Figure 3.**

QD loading capacity and protection of siRNA molecules against nuclease degradation determined by gel electrophoresis. (a) Number of siRNAs that can be immobilized onto a QD. 10 pmol of siRNA was mixed with QDs of various molar ratios (0, 1, 10, 20, 30, 40, and 50). FITC-labeled siRNAs are invisible for siRNA/QD ratios of 1 and 10. However, as the quantity of QDs reduces, free siRNAs (unbound) are clearly detectable, indicating that approximately 10 copies of siRNA will saturate the surface of QDs. For the siRNA delivery experiment discussed below, siRNA/QD ratio of 1 was used because the complexes maintain highly positively charged for cell binding and efficiently rupture endosomes. (b) Free siRNA and QD-siRNA were treated with ribonuclease and the intact siRNA was quantified with



electrophoresis. SDS was used to release siRNA from the carrier QD after the nuclease treatment. Lane 1 and 2 (left to right) shows that SDS causes siRNA band broadening. Free siRNAs are completely digested by nuclease (lane 3). Lane 4 and 5 show that siRNA are undetectable if SDS is not used to release siRNA from the surface of QDs regardless whether siRNA is treated with nuclease. Lane 6 and 7 show the difference of nuclease-treated or non-treated siRNAs after releasing from the surface of QDs. The results show that when free siRNA are completely degraded, approximately 75% of the siRNA on the QD surface are intact.

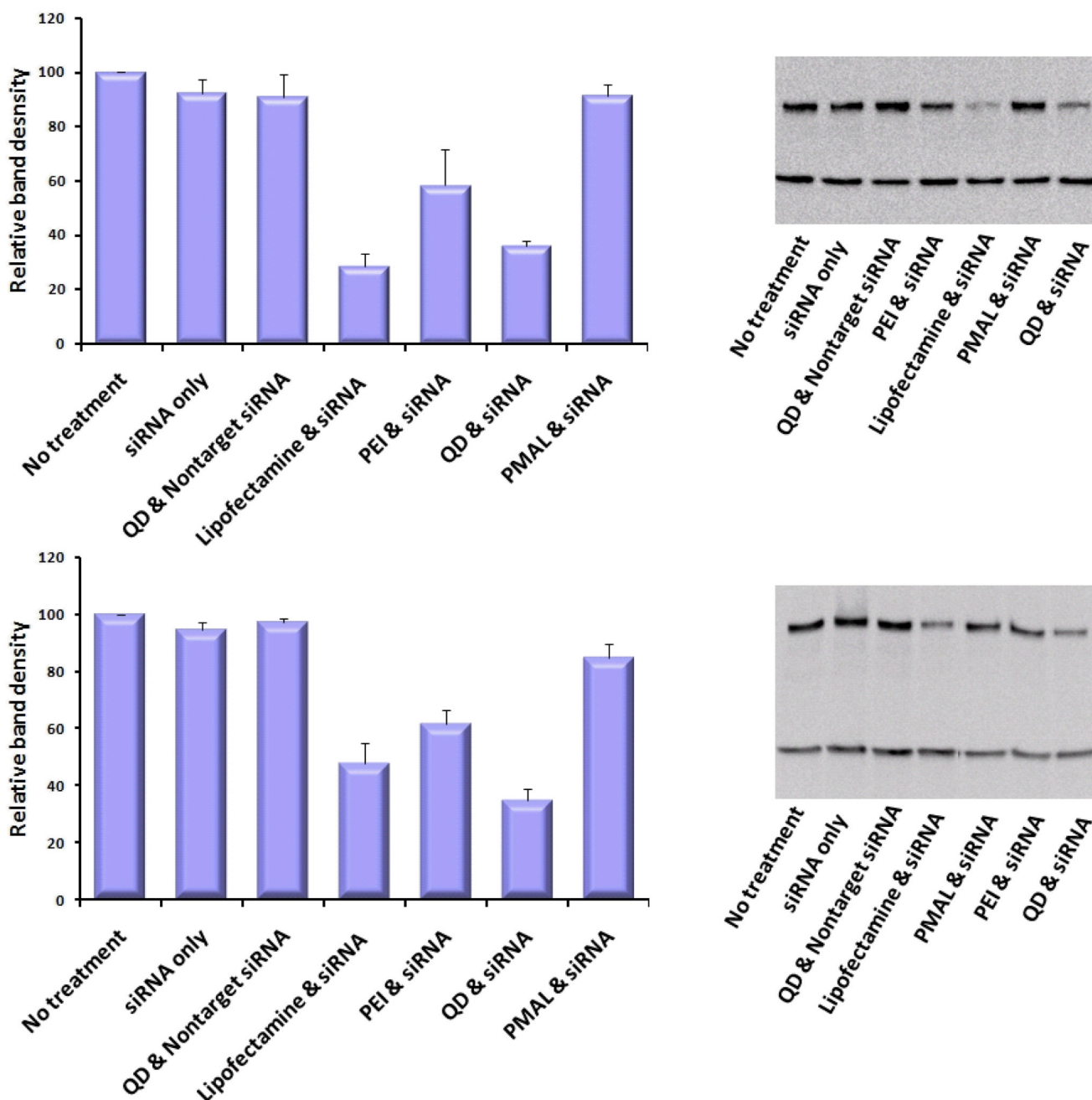


**Figure 4.**

Gene silencing efficiency of siRNA targeting Her-2 using QD-PMAL compared with the classic transfection agents, Lipofectamine and PEI. (a) Under serum-free condition, western blot (right panel) show the level of Her-2 expression was reduced to  $36\% \pm 2\%$  by QD-PMAL, to  $29\% \pm 5\%$  by Lipofectamine, and to  $58\% \pm 13\%$  by PEI (QD-PMAL and Lipofectamine work better than PEI). (b) In complete serum, the level of Her-2 expression was reduced to  $35\% \pm 4\%$  by QD-PMAL, to  $48\% \pm 7\%$  by Lipofectamine, and to  $62\% \pm 5\%$  by PEI. The QD-PMAL efficiency is not significantly affected, but that of Lipofectamine decreases dramatically.

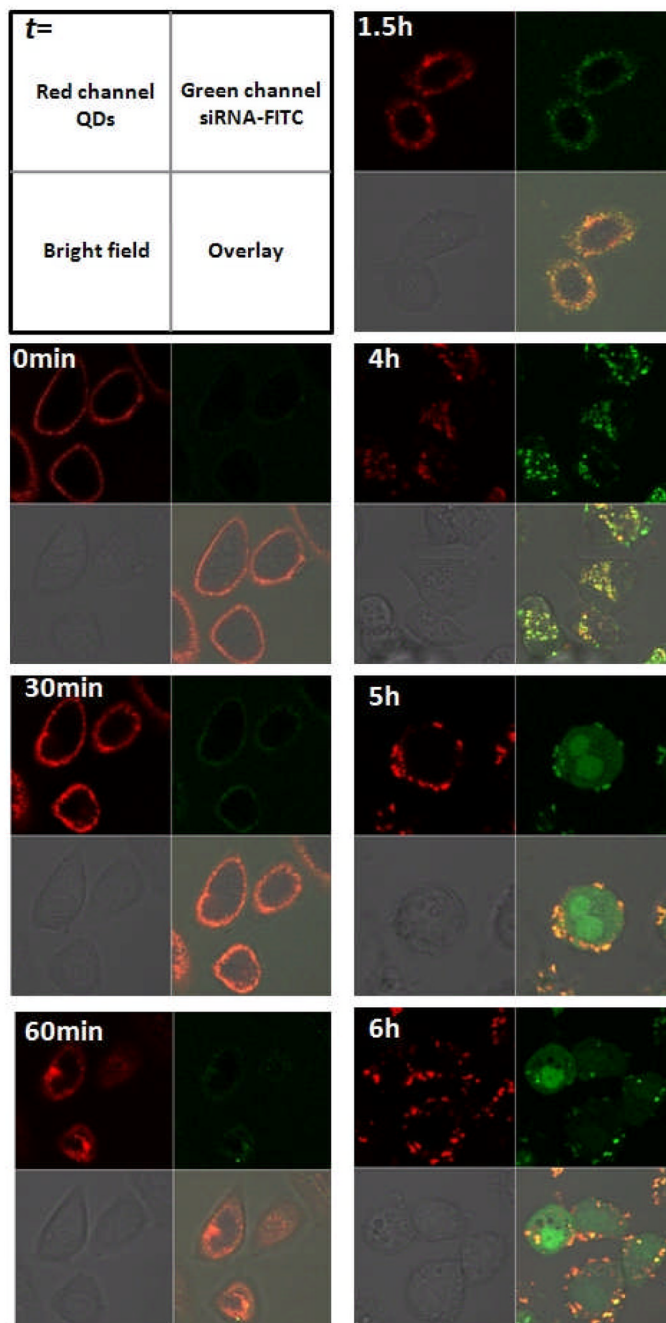


**Figure 5.** Time lapse fluorescence imaging of QD-siRNA complexes and their transport in living cells. QD-siRNA adsorbed onto cell surface immediately after they were added into the cell culture. QD-siRNA entered cells in less than 1 hour incubation time. The green fluorescence from FITC-labeled siRNA started to appear at incubation time of 1.5 hours indicating siRNA separation from QD. The green fluorescence increased over time and at approximately 5 hours, the siRNA were distributed evenly in cells instead of showing a punctuate structure, suggesting efficient endosomal escape.

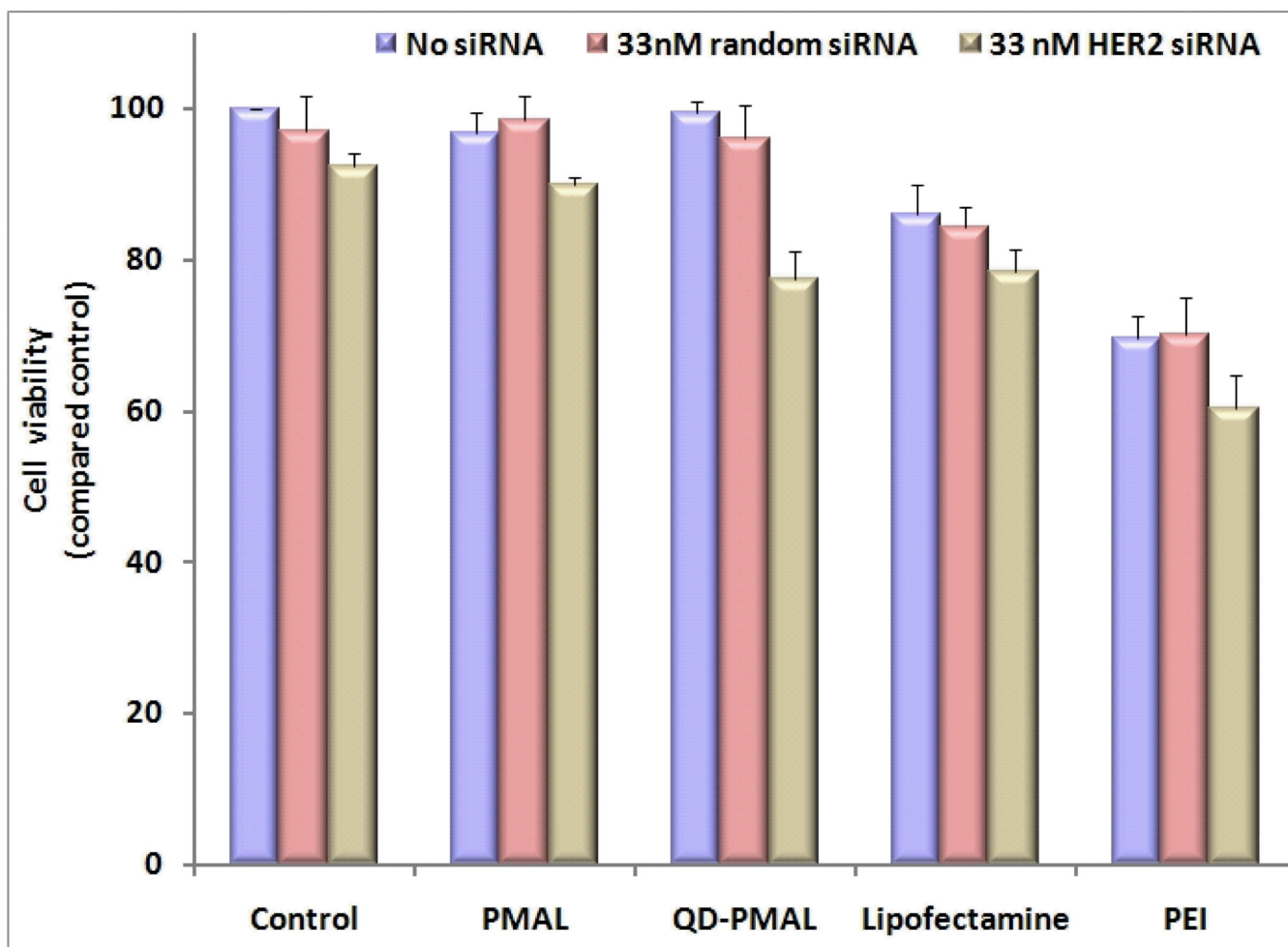


**Figure 6.** Cellular toxicity of QD-PMAL compared with Lipofectamine and PEI at their optimal transfection efficiencies. In the absence of siRNA targeting Her-2 (blue bars) and in the presence of a scramble siRNA sequence (purple bars), the PMAL-coated QDs were nearly non-toxic to SK-BR-3 cells, significantly better than Lipofectamine and PEI. When 33nM Her2-siRNA were used (brown bars), QD-PMAL-siRNA reduced the cell viability by 21.7% because knockdown of Her-2 gene in SK-BR-3 cells inhibits cell proliferation and induces apoptosis. This study shows that QD-PMAL has very low toxicity to cells yet still delivers siRNA efficiently.